PERGAMON

International Journal of Solids and Structures 37 (2000) 7127–7142

INTERNATIONAL JOURNAL OF SOLIDS and STRUCTURES

www.elsevier.com/locate/ijsolstr

The analysis of shear banding with a dislocation based gradient plasticity model

L.J. Sluys [a,*], Y. Estrin [b]

[a] *Department of Civil Engineering and Geosciences, Delft University of Technology, P.O. Box 5048, 2600 GA Delft, Netherlands*
[b] *Department of Mechanical and Materials Engineering, University of Western Australia, Nedlands, WA 6907, Australia*

Received 10 November 1999

Abstract

A microstructural approach to the incorporation of gradient terms in a single crystal plasticity theory is discussed. A diffusion term that represents cross-slip of dislocations is included in the evolution equations for dislocation densities. A coupling between microscale and macroscale is provided by the dislocation based gradient plasticity model. An algorithmic treatment of the model is given. The effect of the diffusion-like term in the constitutive relation on the resulting formation of localized shear modes is studied. An analysis of a plane strain strip in tension oriented for multiple slip is presented. The effect of the dislocation 'diffusivity' on the shear band thickness is analysed. © 2000 Elsevier Science Ltd. All rights reserved.

Keywords: Shear banding; Plasticity model; Dislocation

1. Introduction

The analysis of localized shear modes in engineering materials requires the use of constitutive models, which take spatial coupling into account. Spatial coupling terms represent the microstructure and the microstructural processes that take place during deformation. In the literature this problem is approached from different points of view. A phenomenological approach is the definition of a so-called higher-order continuum in which the higher-order spatial derivatives reflect, in a heuristic way, the microstructure and the micro-structural processes. Examples are nonlocal models, gradient plasticity models and micro-polar models (Aifantis, 1984; Pijaudier-Cabot and Bažant, 1987; Lasry and Belytschko, 1988; Mühlhaus and Aifantis, 1991; Sluys, 1992; de Borst et al., 1993; Sluys et al., 1993). These models (i) introduce a length-scale parameter, (ii) keep the mathematical problem well posed and (iii) remove mesh-size and mesh-orientation dependence in the computational analysis of shear banding. An alternative approach is to start off from the microstructure of a material and derive a continuum formulation by homogenization techniques. Higher-order terms then appear naturally, but they do not necessarily have the same stabilizing

* Corresponding author. Tel.: +31-15-2782728; fax: +31-15-2611465.
E-mail address: l.j.sluys@ct.tudelft.nl (L.J. Sluys).

0020-7683/00/$ - see front matter
PII: S0020-7683(99)00331-5

effect on the formation of localized shear modes as the models mentioned above (Chang and Gao, 1995; Askes et al., 1999).

In this article, we consider gradient plasticity models because of their efficient capabilities with respect to the computational modelling of localized shearing. However, the conventional models cited above have two major drawbacks. First, it is still unclear whether this characteristic length-scale parameter can be measured in a direct or indirect way. Second, the higher-order spatial derivative terms are generally included at a macrolevel and a direct link with the microstructure is lacking. In other words, the origin of the higher-order terms cannot be related to micro-mechanisms that contribute to the spatial coupling effect (it should be mentioned, however, that the higher-order models derived by homogenization techniques do not suffer from this shortcoming). To overcome this deficiency, a gradient plasticity theory with a sound micromechanical basis should be developed. We will do this for a single crystal material, where at microscale localization manifests itself by the occurrence of slip lines produced by dislocations in the crystal lattice. Macroscopic shear band formation in the crystal is a consequence of these microstructural processes.

As for the broad range of conditions, dislocations are the true carriers of plastic deformation, models were formulated in which gradient terms related to dislocation motion were included to account for the spatial interaction, e.g. Walgraef and Aifantis (1985), Mühlhaus and Boland (1991), Estrin and Mühlhaus (1996), Fleck and Hutchinson (1997) and Gao et al. (1999). In the present article, dislocation glide and cross-slip will be shown to provide a spatial coupling mechanism through first-order and second-order gradient terms. The model is embedded in a standard single crystal plasticity framework, which is described in Section 2. The dislocation based gradient plasticity model is outlined in Section 3 for the case of double slip and for multiple slip in an f.c.c. crystal. The algorithmic aspects for the gradient model are discussed in Section 4. The problem to be solved is a coupled problem in which a mechanical equation representing the single crystal model is used together with a reaction-diffusion type equation describing the nonlocal dislocation motion on specific slip systems. The capabilities of the dislocation based gradient model are demonstrated by considering a strip in axial tension in Section 5.

2. Crystal plasticity – constitutive framework

Deformation of a single crystal is assumed to arise from two main mechanisms: (i) the dislocation motion on active-slip systems and (ii) the distortion of the crystal lattice. The kinematic scheme for a finite deformation together with a constitutive formulation for a single crystal is presented for example in Rice (1971), Asaro (1983) and Peirce et al. (1983).

Application of a multiplicative decomposition (Lee, 1969) of the deformation gradient $\mathbf{F}$ gives

$$\mathbf{F} = \mathbf{F}^{\mathrm{e}}\mathbf{F}^{\mathrm{p}}, \tag{1}$$

where the elastic part $\mathbf{F}^{\mathrm{e}}$ describes the stretching and rotation of the lattice and the plastic part $\mathbf{F}^{\mathrm{p}}$ defines the cumulative effect of the dislocation motion. A slip system α is specified by the vectors $\bar{\mathbf{s}}^{\alpha}$ and $\bar{\mathbf{m}}^{\alpha}$ defined in an intermediate configuration as the corresponding slip direction and slip plane normal, respectively. When the single crystal undergoes deformation, the lattice stretches and rotates and the slip system α in the updated configuration is governed by

$$\mathbf{s}^{\alpha} = \mathbf{F}^{\mathrm{e}}\bar{\mathbf{s}}^{\alpha}, \tag{2}$$

$$\mathbf{m}^{\alpha} = \bar{\mathbf{m}}^{\alpha}(\mathbf{F}^{\mathrm{e}})^{-1}. \tag{3}$$

Since $\bar{\mathbf{s}}^{\alpha}$ and $\bar{\mathbf{m}}^{\alpha}$ are orthogonal in the undeformed lattice, so are $\mathbf{s}^{\alpha}$ and $\mathbf{m}^{\alpha}$ in the deformed lattice.

Differentiation of Eq. (1) gives the velocity gradient

$$\dot{\mathbf{F}}\mathbf{F}^{-1} = \dot{\mathbf{F}}^{\mathrm{e}}(\mathbf{F}^{\mathrm{e}})^{-1} + \mathbf{F}^{\mathrm{e}}\dot{\mathbf{F}}^{\mathrm{p}}(\mathbf{F}^{\mathrm{p}})^{-1}(\mathbf{F}^{\mathrm{e}})^{-1} \tag{4}$$

in which a superimposed dot denotes a derivative with respect to time. The first and the second terms in Eq. (4) represent the elastic and the plastic part of the velocity gradient. Because plastic deformation is assumed to occur only by shearing on the slip systems we have

$$\mathbf{F}^{\mathrm{e}}\dot{\mathbf{F}}^{\mathrm{p}}(\mathbf{F}^{\mathrm{p}})^{-1}(\mathbf{F}^{\mathrm{e}})^{-1} = \sum_{\alpha} \dot{\gamma}^{\alpha}\mathbf{s}^{\alpha} \otimes \mathbf{m}^{\alpha} \tag{5}$$

with $\dot{\gamma}^{\alpha}$ denoting the slip strain rate. Using Eqs. (2) and (3), Eq. (5) can be rewritten to yield the flow rule given in Rice (1971)

$$\dot{\mathbf{F}}^{\mathrm{p}}(\mathbf{F}^{\mathrm{p}})^{-1} = \sum_{\alpha} \dot{\gamma}^{\alpha}\bar{\mathbf{s}}^{\alpha} \otimes \bar{\mathbf{m}}^{\alpha}. \tag{6}$$

We introduce the resolved shear stress on system α, τ^{α}, which is work conjugate to the slip strain rate $\dot{\gamma}^{\alpha}$, via

$$\tau^{\alpha} = \mathbf{s}^{\alpha}\boldsymbol{\tau}\mathbf{m}^{\alpha}, \tag{7}$$

where $\boldsymbol{\tau}$ is the Kirchhoff stress (for derivation see Asaro (1983)). To relate the rate of shear deformation to the resolved shear stress τ on a slip system α, we make use of a viscous power-law of the form (Cuitiño and Ortiz, 1992)

$$\dot{\gamma}^{\alpha} = \begin{cases} \dot{\gamma}_0^{\alpha}[(\tau^{\alpha}/g^{\alpha})^{1/m} - 1] & \text{if } \tau^{\alpha} > g^{\alpha}, \\ 0, & \text{otherwise} \end{cases} \tag{8}$$

in which $\dot{\gamma}_0^{\alpha}$ is a reference shear-strain rate, m is the strain rate sensitivity exponent and g^{α} is the yield stress on slip system α. The hardening of the crystal material is specified by the evolution of the yield stress g^{α}. A slip system α is considered as active if τ^{α} is greater than the threshold g^{α}. In macroscopic hardening models, the evolution with time of the yield stress on the slip strain rate is generally defined as

$$\dot{g}^{\alpha} = \sum_{\beta} h^{\alpha\beta}\dot{\gamma}^{\beta}. \tag{9}$$

The strain hardening matrix $h^{\alpha\beta}$ is dependent on an internal variable, which evolves with γ^{α}, and local interaction between slip systems with different orientations is taken into account via the off-diagonal terms in $h^{\alpha\beta}$. In the microscopic model, we present in the next paragraph, a dependence of $h^{\alpha\beta}$ on the dislocation density, which plays the role of an internal variable, will be derived.

3. Dislocation model for hardening

First, we will analyse an idealized model for dislocation motion in a double-conjugate slip format introduced by Asaro (1983). A dislocation density related extension of the model was carried out. In this Section, this extended model will be presented following Estrin et al. (1998). Further, we generalize the model to include the case of multiple slip. First, we consider a crystal with two slip systems whose slip directions $\mathbf{s}^{\alpha}$ and slip plane normals $\mathbf{m}^{\alpha}$ are assumed to lie in one plane. The expression for the yield stress is taken in the form (Estrin et al., 1998)

$$g^1 = aGb\sqrt{\rho^2}, \tag{10a}$$

$$g^2 = aGb\sqrt{\rho^1}, \tag{10b}$$

where G is the shear modulus, b is the magnitude of the dislocation Burgers vector, a is a constant and ρ^{α} is the density of dislocations moving on the slip system α, with $\alpha = 1, 2$ for double-conjugate slip. In the

model, no distinction is made between mobile and immobile dislocations. According to Eqs. (10a) and (10b), the yield stress for one slip system is assumed to be determined by the dislocation density on the other slip system only. In other words, latent hardening is included while self-hardening of a particular slip system is neglected. Also, the reference shear-strain rate $\dot{\gamma}_0$ is related to the dislocation density via

$$\dot{\gamma}_0^\alpha = k\rho^\alpha, \quad \alpha = 1,2, \tag{11}$$

where k is a constant.

The evolution of the dislocation density is defined by

$$\dot{\rho}^\alpha = \dot{\gamma}^\alpha\left(J\sqrt{\rho^\beta} - K\rho^\alpha\right), \quad \alpha \neq \beta \in 1,2 \tag{12}$$

suggesting that the mean free path of dislocations of a slip system is determined by the dislocation density of the other slip system. The recovery process is assumed to involve two dislocations of the same slip system giving rise to the negative term on the right-hand side of Eq. (12). The coefficient J in the athermal dislocation storage term is considered to be a constant whereas the coefficient K in the thermally activated recovery term is temperature and strain rate dependent (Estrin, 1996).

Gradient terms are included by introducing the dislocation flux $\mathbf{j}^\alpha$, i.e. by replacing Eq. (12) with the continuity equation

$$\dot{\rho}^\alpha = \dot{\gamma}^\alpha\left(J\sqrt{\rho^\beta} - K\rho^\alpha\right) - \operatorname{div}\mathbf{j}^\alpha, \quad \alpha \neq \beta. \tag{13}$$

The fluxes are best calculated in the coordinate systems associated with the slip planes and their normals. For example, consider the slip system 1 (Fig. 1). In the coordinate system ($\mathbf{s}^1$, $\mathbf{m}^1$), the flux component along $\mathbf{s}^1$ is associated with the dislocation glide and is given by

$$j_s^1 = \rho^1 v^1 = \dot{\gamma}^1/b, \tag{14}$$

where v^1 is the dislocation glide velocity. To calculate the flux component in the perpendicular direction (m^1), we consider dislocation exchange between neighbouring slip planes via the double cross-slip mechanism (Brechet and Louchet, 1988; Estrin, 1988; Kubin and Poirier, 1988). Therefore, the frequency ω of the cross-slip events between the neighbouring slip planes and the spacing d between the active slip planes are introduced. If we assume that the density of dislocations leaving a glide plane for one of its nearest neighbouring planes is given by the product of ω and the dislocation density in the plane, one finds that in the continuum limit, (Brechet and Louchet, 1988; Estrin, 1988; Kubin and Poirier, 1988) the component of the flux in the direction of m^1 is given by

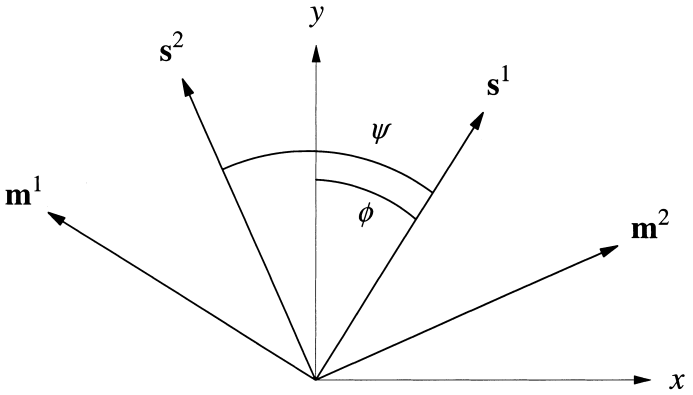

Fig. 1. Geometry of slip with respect to the laboratory coordinate system.

$$j_m^1 = -D\frac{\partial \rho^1}{\partial m^1} \tag{15}$$

in which $D = \omega d^2$. Thus, the dislocation flux on slip system 1 can be expressed as

$$\mathbf{j}^1 = j_s^1 \mathbf{s}^1 + j_m^1 \mathbf{m}^1 \tag{16}$$

with j_s^1 and j_m^1 given by Eqs. (14) and (15). The divergence of the dislocation flux is then represented by (Estrin et al., 1998)

$$\operatorname{div}\mathbf{j}^1 = \frac{1}{b}\frac{\partial \dot{\gamma}^1}{\partial s^1} - D\frac{\partial^2 \rho^1}{\partial (m^1)^2}. \tag{17}$$

It is seen that the cross-slip effect leads to a term in the direction normal to the slip plane which is formally similar to a diffusion term. The 'diffusivity' D determined by the cross-slip frequency and the active slip plane spacing introduces a length-scale, which is important for the shear band simulations as will be demonstrated later. The significance of the relation $D = \omega d^2$ is that it establishes a connection between gradient plasticity and the micromechanical mechanism, viz. the cross-slip characteristics. A frame for the evaluation of the cross-slip parameters is set by the ideas of Escaig (1968).

Substituting Eq. (17) into Eq. (13) and using the transformation from the coordinate system connected to the slip system (s^1, m^1) with the laboratory coordinates (x,y) one obtains

$$\begin{aligned}\dot{\rho}^1 = {} & \dot{\gamma}^1\left(J\sqrt{\rho^2} - K\rho^1\right) - \frac{\sin\phi}{b}\frac{\partial \dot{\gamma}^1}{\partial x} - \frac{\cos\phi}{b}\frac{\partial \dot{\gamma}^1}{\partial y} \\ & + D\left(\cos^2\phi\frac{\partial^2 \rho^1}{\partial x^2} - 2\sin\phi\cos\phi\frac{\partial^2 \rho^1}{\partial x \partial y} + \sin^2\phi\frac{\partial^2 \rho^1}{\partial y^2}\right)\end{aligned} \tag{18}$$

in which ϕ is the angle between the coordinate axis y and the slip direction s^1. Similarly, the equation for the dislocation density ρ^2 reads

$$\begin{aligned}\dot{\rho}^2 = {} & \dot{\gamma}^2\left(J\sqrt{\rho^1} - K\rho^2\right) - \frac{\sin(\psi-\phi)}{b}\frac{\partial \dot{\gamma}^2}{\partial x} - \frac{\cos(\psi-\phi)}{b}\frac{\partial \dot{\gamma}^2}{\partial y} \\ & + D\left(\cos^2(\psi-\phi)\frac{\partial^2 \rho^2}{\partial y^2} - 2\sin(\psi-\phi)\cos(\psi-\phi)\frac{\partial^2 \rho^2}{\partial x \partial y} + \sin^2(\psi-\phi)\frac{\partial^2 \rho^2}{\partial x^2}\right)\end{aligned} \tag{19}$$

in which ψ is the angle between the two slip planes and $\psi - \phi$ is the angle between the slip plane of slip system 2 and the coordinate axis y (cf. Fig. 1).

Relation (9) with the hardening moduli is affected by the inclusion of higher-order gradient terms. Differentiation of Eqs. (10a) and (10b) with respect to time yields

$$\dot{g}^1 = \frac{aGb}{2}\frac{\dot{\rho}^2}{\sqrt{\rho^2}}, \tag{20a}$$

$$\dot{g}^2 = \frac{aGb}{2}\frac{\dot{\rho}^1}{\sqrt{\rho^1}}. \tag{20b}$$

Substitution of the evolution equations for the dislocation densities, Eqs. (18) and (19), into Eqs. (20a) and (20b) yields

$$\dot{g}^1 = \frac{aGb}{2}\left(\dot{\gamma}^2(J\sqrt{\rho^1/\rho^2} - K\sqrt{\rho^2}) - \frac{1}{b\sqrt{\rho^2}}\left(\sin\phi\frac{\partial\dot{\gamma}^1}{\partial x} + \cos\phi\frac{\partial\dot{\gamma}^1}{\partial y}\right) + \frac{D}{\sqrt{\rho^2}}\left(\cos^2\phi\frac{\partial^2\rho^1}{\partial x^2} - 2\sin\phi\cos\phi\frac{\partial^2\rho^1}{\partial x\,\partial y} + \sin^2\phi\frac{\partial^2\rho^1}{\partial y^2}\right)\right), \tag{21}$$

$$\dot{g}^2 = \frac{aGb}{2}\left(\dot{\gamma}^1(J\sqrt{\rho^2/\rho^1} - K\sqrt{\rho^1}) - \frac{1}{b\sqrt{\rho^1}}\left(\sin(\psi-\phi)\frac{\partial\dot{\gamma}^2}{\partial x} + \cos(\psi-\phi)\frac{\partial\dot{\gamma}^2}{\partial y}\right) + \frac{D}{\sqrt{\rho^1}}\left(\cos^2(\psi-\phi)\frac{\partial^2\rho^2}{\partial y^2} - 2\sin(\psi-\phi)\cos(\psi-\phi)\frac{\partial^2\rho^2}{\partial x\,\partial y} + \sin^2(\psi-\phi)\frac{\partial^2\rho^2}{\partial x^2}\right)\right) \tag{22}$$

from which the hardening matrix can be computed according to

$$h^{\alpha\beta} = \frac{\partial\dot{g}^\alpha}{\partial\dot{\gamma}^\beta} = \begin{bmatrix} \frac{\partial\dot{g}^1}{\partial\dot{\gamma}^1} & \frac{\partial\dot{g}^1}{\partial\dot{\gamma}^2} \\ \frac{\partial\dot{g}^2}{\partial\dot{\gamma}^1} & \frac{\partial\dot{g}^2}{\partial\dot{\gamma}^2} \end{bmatrix}. \tag{23}$$

The dislocation model is not only used for double-conjugate slip but can also be generalized to the case of a face-centred cubic (f.c.c.) crystal containing 12 slip systems. Therefore, the expression for the yield stress, Eqs. (10a) and (10b), and the dislocation density evolution equation (12) need to be modified. A straightforward extension reads

$$g^\alpha = \alpha Gb\sqrt{\sum_{\beta\neq\alpha}\rho^\beta}, \tag{24}$$

$$\dot{\rho}^\alpha = \dot{\gamma}^\alpha\left(J\sqrt{\sum_{\beta\neq\alpha}\rho^\beta} - K\rho^\alpha\right) \tag{25}$$

in which differences in the interaction between different slip systems (Franciosi and Zaoui, 1982) are neglected. An extension with gradient terms is obtained using the same procedure as above.

The model presented has the following features: Strain softening associated with local lattice rotation may give rise to strain localization at later stages of deformation when it can no longer be restrained by strain hardening, cf. Asaro (1983), Peirce et al. (1983), and Balke and Estrin (1994). In the present model, this effect decreases because of the gradient terms, which force the evolving dislocation densities to saturate. Due to the positive sign of D the "diffusion-like" terms in the equations will act against strain localization and will thus play a stabilizing role.

4. Algorithmic aspects

We deal with a coupled problem on the basis of a mechanical model for single crystal behaviour outlined in Section 2. The model conforms with the general constitutive framework for single crystal plasticity as discussed by Peirce et al. (1983). The update of the slip strains and the resolved shear stresses can be computed from the updated state as a function of the deformation gradient $\mathbf{F}$. Eqs. (1) and (6)–(9) can be written as a set with the unknown incremental slip strain $\Delta\gamma^\alpha$. The system can be solved with a Newton–Raphson iteration performed at integration point level, cf. Cuitiño and Ortiz (1992). From the update

algorithm a consistent tangent can be derived, which is non-symmetric (see also Moran et al. (1990)). In combination with a Newton–Raphson procedure, this warrants a quadratic convergence of the global set of equations (this is only true when the set of active-slip systems between two iterations does not change). For the determination of the set of active slip systems, an iterative algorithm is used in which the incremental slip strains $\Delta\gamma^\alpha$ are computed for the active slip systems in the previous time step. The active set changes if on one of the inactive systems the resolved shear stress exceeds the shear flow stress ($\tau^\alpha > g^\alpha$) (if this occurs for more than one system, only the most loaded system, i.e. the one with the maximum $\tau^\alpha - g^\alpha$, is added). In the new set of active systems, the slip strains can be recomputed. When the slip pattern remains unchanged, the searching algorithm is converged for this particular integration point. A procedure for determining the set of active slip systems is discussed by Cuitiño and Ortiz (1992).

Next, a finite element formulation of the diffusion-reaction equations (18) and (19) can be derived for a simplified case. For the sake of simplicity, the case of double slip is assumed in combination with *isotropic dislocation diffusion*. The problem is then reduced to the set of equations (see also Sluys et al. (1995) and Estrin et al. (1998))

$$\dot{\rho}^\alpha = \dot{\gamma}^\alpha(J\sqrt{\rho^\beta} - K\rho^\alpha) + D\nabla^2\rho^\alpha, \quad \alpha \neq \beta \tag{26}$$

in which the Laplacian $\nabla^2\rho^\alpha = \partial^2\rho^\alpha/\partial x^2 + \partial^2\rho^\alpha/\partial y^2$ is introduced and dislocation glide related spatial derivatives are not taken into account. A finite element solution of the reaction-diffusion equation is derived by means of a weak form according to

$$\int_V \delta\rho^\alpha \left[\dot{\rho}^\alpha - \dot{\gamma}^\alpha(J\sqrt{\rho^\beta} - K\rho^\alpha) - D\nabla^2\rho^\alpha\right] \mathrm{d}V = 0. \tag{27}$$

We use Green's theorem to rewrite the diffusion term in Eq. (27)

$$\int_V \delta\rho^\alpha \nabla(D\nabla\rho^\alpha)\,\mathrm{d}V = -\int_V (\nabla\delta\rho^\alpha)^{\mathrm{T}}(D\nabla\rho^\alpha)\,\mathrm{d}V + \int_S \delta\rho^\alpha (D\nabla\rho^\alpha)^{\mathrm{T}}\mathbf{n}\,\mathrm{d}S \tag{28}$$

with $\mathbf{n}$ a vector perpendicular to the boundary. The boundary term on the right-hand side vanishes if the dislocation flux at the boundary is zero

$$(\mathbf{j}^\alpha)^{\mathrm{T}} \cdot \mathbf{n} = (D\nabla\rho^\alpha)^{\mathrm{T}} \cdot \mathbf{n} = \mathbf{0}. \tag{29}$$

The remaining system is discretized according to

$$\rho^\alpha(\mathbf{x}, t) = \mathbf{h}^{\mathrm{T}}\mathbf{p}^\alpha, \tag{30}$$

$$\nabla\rho^\alpha(\mathbf{x}, t) = \mathbf{B}\mathbf{p}^\alpha, \tag{31}$$

in which $\mathbf{p}^\alpha$ are the nodal dislocation densities and $\mathbf{h}$ the shape functions. The matrix $\mathbf{B}$ contains the derivatives of the shape functions with respect to the reference configuration. For double slip $\mathbf{p}^\alpha$ contains two degrees of freedom per node and for an f.c.c. crystal it has 12 degrees of freedom per node. The semi-discretized reaction-diffusion equation reads

$$\mathbf{M}\dot{\mathbf{p}}^\alpha + \mathbf{K}\mathbf{p}^\alpha = \mathbf{s}^\alpha \tag{32}$$

with

$$\mathbf{M} = \int_V \mathbf{h}\mathbf{h}^{\mathrm{T}}\,\mathrm{d}V, \tag{33}$$

$$\mathbf{K} = \int_V \mathbf{B}^{\mathrm{T}} D\mathbf{B}\,\mathrm{d}V, \tag{34}$$

$$\mathbf{s}^{\alpha} = \int_V \mathbf{h}\left(\dot{\gamma}^{\alpha}\left(J\sqrt{\rho^{\beta}} - K\rho^{\alpha}\right)\right) \mathrm{d}V, \quad \alpha \neq \beta. \tag{35}$$

Time integration is carried out by considering Eq. (32) at time $t + \Delta t$

$$\mathbf{M}\dot{\mathbf{p}}^{\alpha}_{t+\Delta t} + \mathbf{K}\mathbf{p}^{\alpha}_{t+\Delta t} = \mathbf{s}^{\alpha}_{t}, \tag{36}$$

$$\mathbf{p}^{\alpha}_{t+\Delta t} = \mathbf{p}^{\alpha}_{t} + \Delta t[(1-\theta)\dot{\mathbf{p}}^{\alpha}_{t} + \theta\dot{\mathbf{p}}^{\alpha}_{t+\Delta t}], \tag{37}$$

where θ is an interpolation parameter. The scheme is fully implicit with $\theta = 1$. Substitution of Eq. (37) into Eq. (36) gives

$$\hat{\mathbf{K}}\mathbf{p}^{\alpha}_{t+\Delta t} = \hat{\mathbf{f}}^{\alpha}_{t} \tag{38}$$

in which

$$\hat{\mathbf{K}} = (1/(\theta\Delta t))\mathbf{M} + \mathbf{K}, \tag{39}$$

$$\hat{\mathbf{f}}^{\alpha}_{t} = \mathbf{s}^{\alpha}_{t} + [(1/(\theta\Delta t))\mathbf{M} - \mathbf{K}]\mathbf{p}^{\alpha}_{t} + ((1-\theta)/\theta)\mathbf{M}\dot{\mathbf{p}}^{\alpha}_{t}. \tag{40}$$

We have a coupled set of equations, including a momentum balance equation with traditional degrees of freedom complemented with a reaction-diffusion equation with two degrees of freedom per node for the case of double-conjugated slip and 12 degrees of freedom per node for an f.c.c. crystal. The problem can be solved by uncoupling the two equations during a time step. First, the reaction-diffusion equations have been solved with input $\mathbf{s}^{\alpha}$ from the previous step. The nodal dislocation densities can be calculated according to the above procedure. Second, the mechanical mesh is evaluated with the updated dislocation densities that determine the yield stress Eqs. (10a) and (10b) and the reference strain rate (Eq. (11)). Both equations are solved implicitly, whereas the treatment of the two meshes is done explicitly.

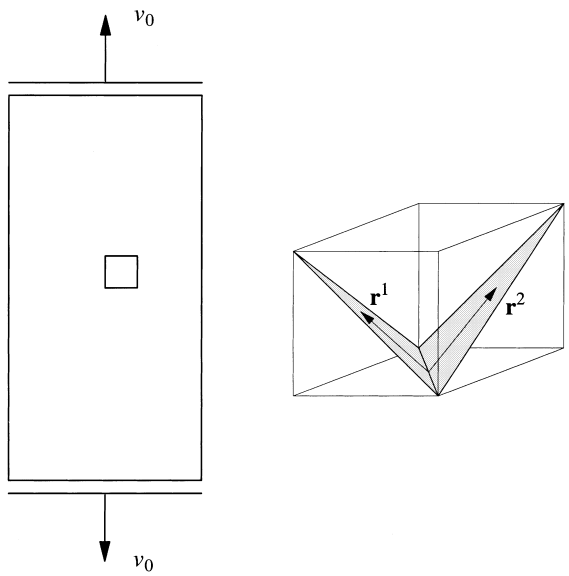

Fig. 2. Plane strain strip in uniaxial tension with an imperfection (left) and f.c.c. crystal orientation (right).

5. Strip in tension

To investigate the behaviour of the gradient plasticity model for dislocation motion in a single crystal a strip in tension is considered. Multiple slip in a rectangular strip of an f.c.c. crystal is analysed for plane strain conditions. Therefore, Eqs. (24) and (25) are used in place of the equations for double-conjugate slip. A 4 mm × 10 mm strip is pulled in tension by applying a constant axial velocity $v_0 = 0.1$ mm/s at the top and the bottom of the specimen (Fig. 2). The two vertical edges of the strip are traction free. The crystal is oriented according to an $(\mathbf{a}_1, \mathbf{a}_2, \mathbf{a}_3) = ([1\,0\,\bar{1}], [0\,1\,0], [1\,0\,1])$ coordinate system which for axial tension results in active-slip on the $(1\,1\,\bar{1})$ plane in the directions $[\bar{1}\,1\,0]$ and $[0\,1\,1]$ with resultant $\mathbf{r}^1$ and on the $(1\,\bar{1}\,\bar{1})$ plane in the directions $[1\,1\,0]$ and $[0\,1\,\bar{1}]$ with resultant $\mathbf{r}^2$ (Fig. 2). The values for the material constants employed are $G = 75\,000$ N/mm^2, $a = 0.3$, $b = 2.5 \times 10^{-7}$ mm, $\rho_0 = 1 \times 10^8$ mm^{-2}, $m = 0.005$, $k = 1/\rho_0$, $K = 10$, $J = 4 \times 10^6$ mm^{-1}, $D/\sqrt{\rho_0} = 2$ mm^3/s. In order to trigger shear banding, a small imperfection (reduction of constant a by 2.5%) is applied slightly to the right of the centre of the strip. Three different meshes were used with 320 (mesh 1), 720 (mesh 2) and 1280 (mesh 3) 6-noded triangular elements.

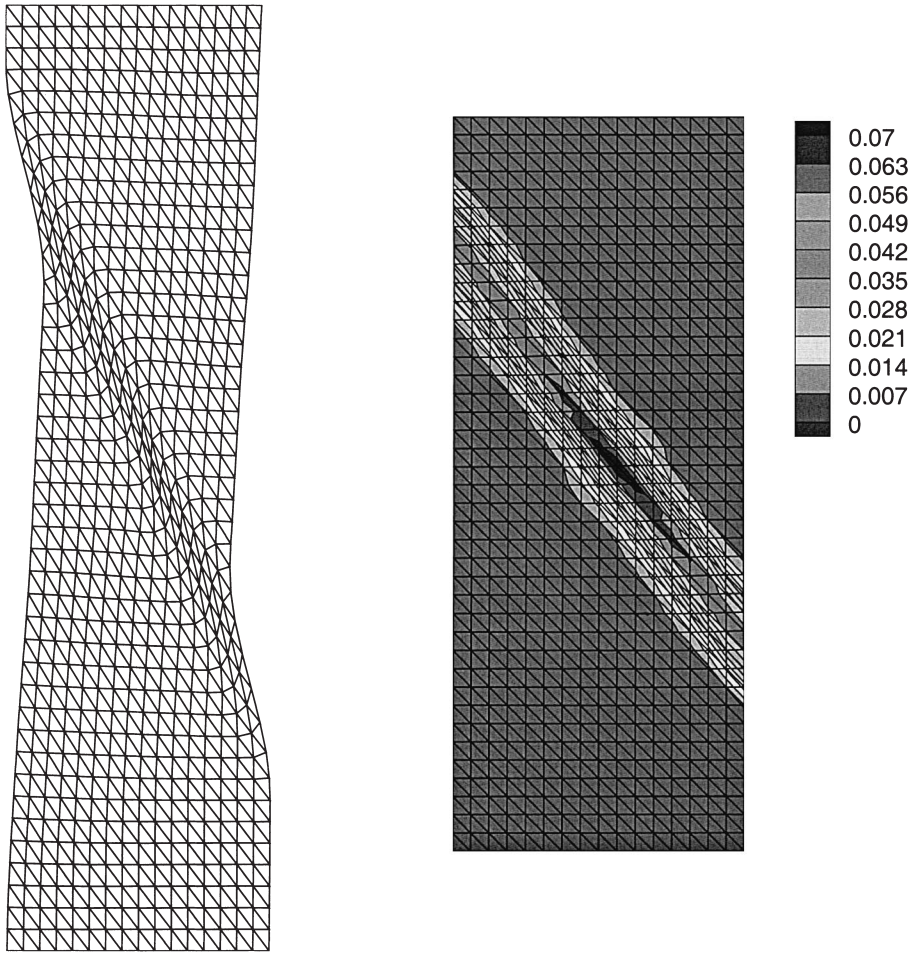

Fig. 3. Strip in tension – results for mesh 3 at $t = 0.1$ s: left – deformed model (deformations multiplied by factor 30), right – total slip strain $\sum \gamma^\alpha$ on active systems.

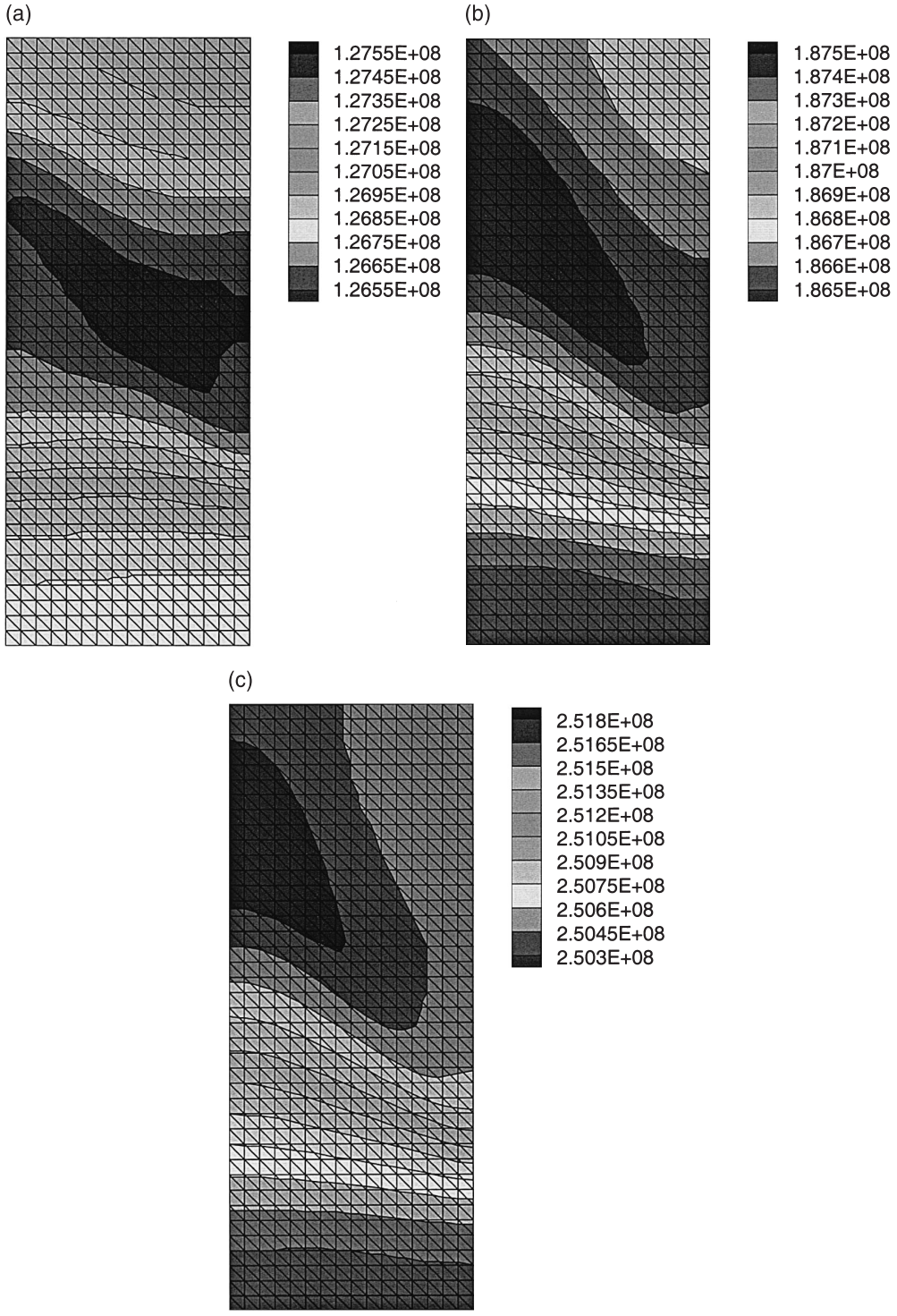

Fig. 4. Dislocation densities at systems $[\bar{1}\,1\,0]$ and $[0\,1\,1]$ on plane $(1\,1\,\bar{1})$ at $t = 0.06$ s (left), $t = 0.08$ s (centre) and $t = 0.10$ s (right).

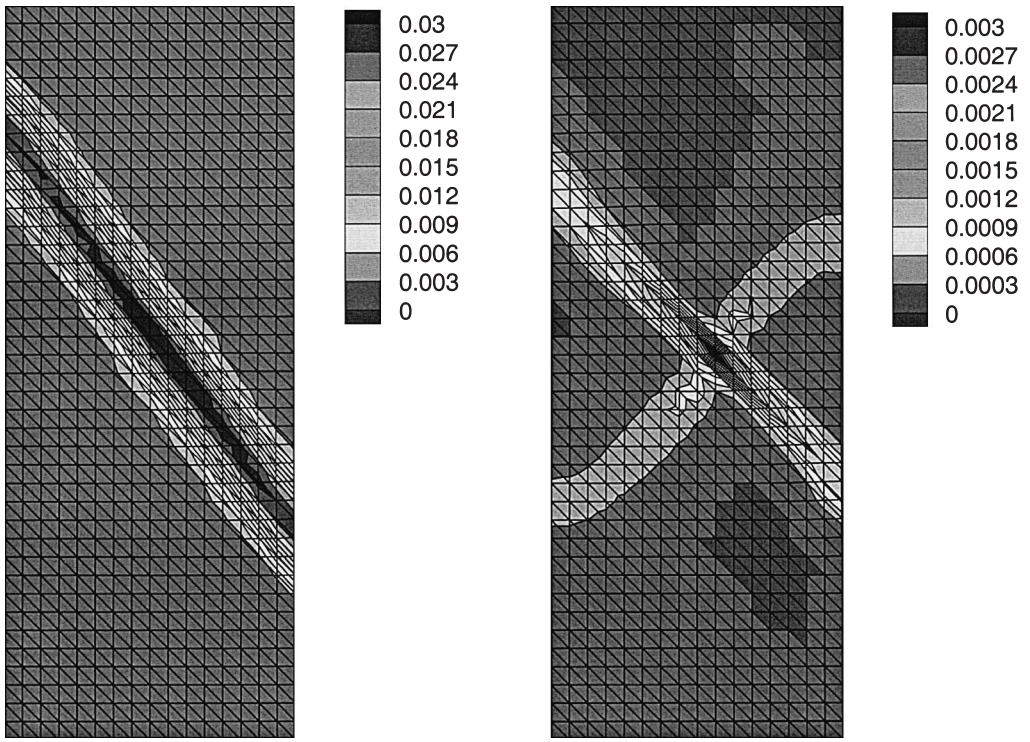

Fig. 5. Slip strains at systems $[\bar{1}\,1\,0]$ and $[0\,1\,1]$ on plane $(1\,1\,\bar{1})$ (left) and systems $[1\,1\,0]$ and $[0\,1\,\bar{1}]$ on plane $(1\,\bar{1}\,\bar{1})$ (right).

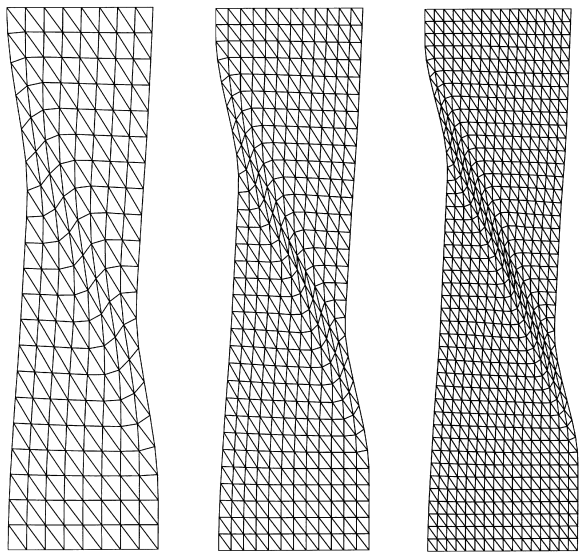

Fig. 6. Deformed model (multiplication factor 30) – mesh 1: 320 elements (left), mesh 2: 720 elements (centre) and mesh 3: 1280 elements (right).

The results after a certain amount of crystallographic slip are shown in Fig. 3. The deformed model shows that one shear band becomes dominant due to the asymmetric location of the imperfection and the structure of the mesh (deformations are multiplied by a factor of 30). The shear band has a specific thickness, which is predominantly set by the material parameters J and D and also by the dimensions of the strip and the boundary conditions. The corresponding sum of the slip strains on the two activated planes (Fig. 2) are also plotted in Fig. 3. The slip strains have peak values in the centre of the shear band. It is obvious that the direction of the shear band is not aligned with the mesh. The contours of the dislocation densities for three consecutive stages of evolution are plotted in Fig. 4. The diffusive property of the model is evident, with the dislocations being spread over the specimen in the course of time. In Fig. 5, the slip activity on the two activated systems is presented separately. A remarkable result is that the combined system $\mathbf{r}^1$ on plane $(1\,1\,\bar{1})$ runs steeper than the resultant $\mathbf{r}^2$ on plane $(1\,\bar{1}\,\bar{1})$ and also a wider band is obtained. By contrast, the system $\mathbf{r}^2$ attracts less deformation (Fig. 5, where the maximum slip strain is smaller by a factor of 10), and therefore, the shear band is dominated by the two systems that are represented by $\mathbf{r}^1$, which can be seen by comparing Figs. 3 and 5.

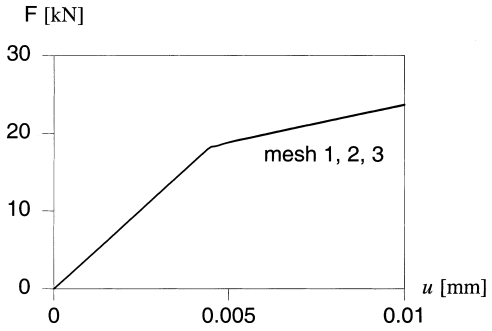

Fig. 7. Load–displacement diagram for different meshes ($0 < t < 0.1$ s).

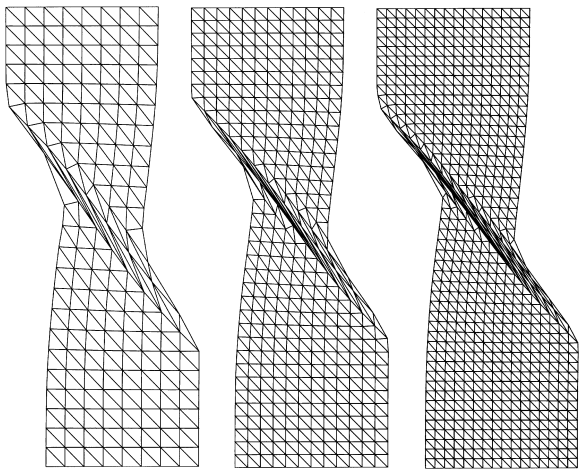

Fig. 8. Deformed model for three meshes at $t = 2.0$ s (no multiplication factor used).

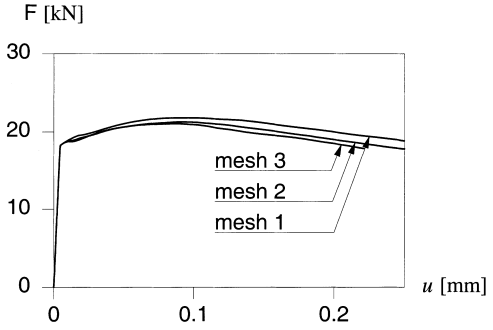

Fig. 9. Load–displacement diagram for different meshes ($0 < t < 2.5$ s).

Further, the sensitivity of the results to the finite element size was investigated. The thickness of the band is slightly over predicted with the coarsest mesh, but the two finer meshes show the same shear banding process (Fig. 6). The load–displacement curves for the three mesh sizes are almost identical (Fig. 7). Thus, even for the coarsest mesh the global comparison of the results does not show a mesh size effect. The same calculations were carried out over a significantly longer time interval. If both ends of the strip are displaced at constant speed for 2.5 s, a 5% deformation is reached. The displacements are plotted in Fig. 8 (without a multiplication factor). Extreme shear banding takes place for all three different meshes used. Now, the load–displacement curves in Fig. 9 show global softening behaviour. Although the material is hardening locally through multiple slip, a global softening behaviour does not induce mesh dependence.

Next, the amount of coupling is varied through the magnitude of the dislocation diffusivity D. Increasing D, widens the shear band, whereas a decrease of D leads to a slightly thinner band (Fig. 10). The final results come from a variation of the athermal coefficient J, which has a similar effect to varying D. A widening of the shear band resulting in more plastic behaviour is found on increasing the value of J, cf.

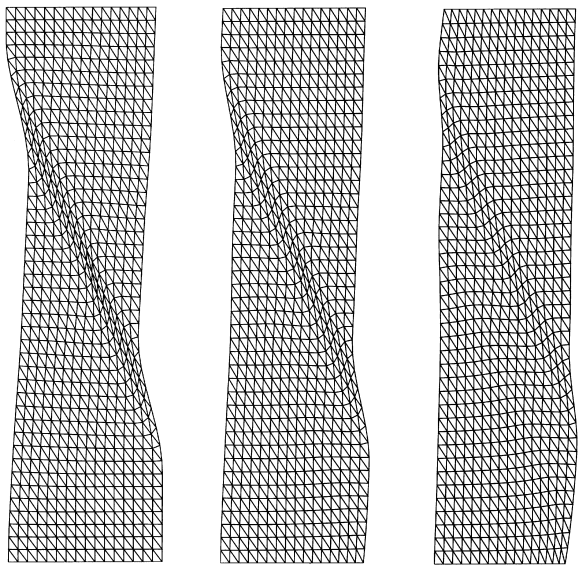

Fig. 10. Variation of dislocation diffusivity: $D/\sqrt{\rho_0} = 2$ mm^3/s (left), $D/\sqrt{\rho_0} = 4$ mm^3/s (centre) and $D/\sqrt{\rho_0} = 8$ mm^3/s (right). Deformed models (multiplication factor of 30) at $t = 0.1$ s.

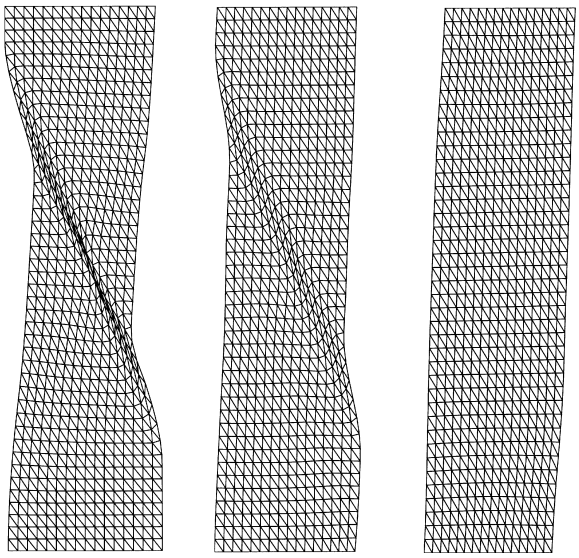

Fig. 11. Variation of athermal coefficient: $J = 0.8 \times 10^6$ mm^{-1} (left), $J = 4.0 \times 10^6$ mm^{-1} (centre) and $J = 20.0 \times 10^6$ mm^{-1} (right). Deformed models (multiplication factor of 30) at $t = 0.1$ s.

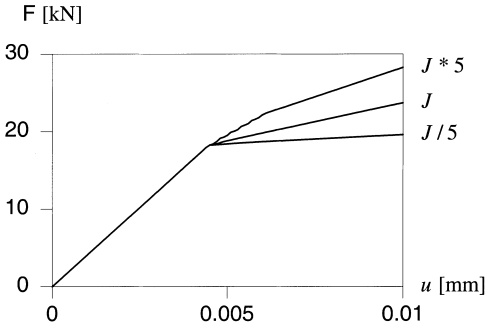

Fig. 12. Load–displacement diagram for analyses with different J values.

Figs. 11 and 12. By contrast, a very sharp shear band (Fig. 11, left) is observed for a smaller value of J ($J/5 = 0.8 \times 10^6$, mm^{-1}), which corresponds to the lowest branch in Fig. 12.

6. Conclusions

A general frame for the introduction of higher-order spatial derivatives in a single crystal plasticity theory was presented. To give the higher-order terms a physical basis, a micro-mechanically motivated gradient plasticity theory developed by Estrin et al. (1998) was used. In this article, the full algorithmic treatment was given and a generalization of the model to include the case of multiple slip was carried out. Dislocation motion on a slip plane by dislocation glide and perpendicular to the slip plane by cross-slip are seen to lead to the spatial coupling effects that cause the higher-order terms. The model was embedded in a standard single crystal plasticity framework. A coupling between macroscale and microscale was thus es-

tablished. This coupled problem involving a mechanical equation for the single crystal and a reaction-diffusion equation for the dislocation densities was solved in a partially decoupled way. The dislocation based gradient plasticity model was used for the analysis of multiple slip in a strip under uniaxial tension under simplifying conditions of isotropic "dislocation diffusion".

Acknowledgements

Valuable contributions of Michael Ortiz and Alan Needleman to the computational aspects of gradient plasticity including dislocations, cf. Sluys et al. (1995), and of Yves Brechet and Alain Molinari to the formulation of the model presented in Section 3, cf. Estrin et al. (1998), are gratefully acknowledged.

References

Aifantis, E.C., 1984. On the microstructural origin of certain inelastic models. J. Engng. Mater. Technol. 106, 326–334.
Asaro, R.J., 1983. Micromechanics of crystals and polycrystals. Adv. Appl. Mech. 23, 1–115.
Askes, H., Suiker, A.S.J., Sluys, L.J., 1999. Dispersion and numerical analysis of higher-order gradient models in homogenized and regularized media. TU Delft report 03.21.1.31.07, Delft University of Technology, Netherlands.
Balke, H., Estrin, Y., 1994. Micromechanical modelling of shear banding. Int. J. Plasticity 10, 133–147.
de Borst, R., Sluys, L.J., Mühlhaus, H.-B., Pamin, J., 1993. Fundamental issues in finite element analyses of localization of deformation. Engng. Comput. 10, 99–121.
Brechet, Y., Louchet, F., 1988. Localization of plastic deformation. In: Kubin, L.P., Martin, G. (Eds.), Non Linear Phenomena in Materials Science. Trans. Tech. Publ, Clausthal, pp. 347–356.
Chang, C.S., Gao, J., 1995. Second-gradient constitutive theory for granular material with random packing structure. Int. J. Solids Struct. 16, 2279–2293.
Cuitiño, A.M., Ortiz, M., 1992. Computational modelling of single crystals. Modelling Simul. Mater. Sci. Engng. 1, 225–263.
Escaig, B., 1968. Sur le glissement devie des dislocations dans la structure cubique a faces centrées. J. de Physique 28, 225–239.
Estrin, Y., 1996. Dislocation density related constitutive modelling. In: Krausz, A.S., Krausz, K. (Eds.), Unified Constitutive Laws of Plastic Deformation. Academic Press, New York, pp. 69–106.
Estrin, Y., 1988. Classification of plastic instabilities by linear stability analysis. In: Kubin, L.P., Martin, G. (Eds.), Non Linear Phenomena in Materials Science. Trans Tech Publ, Clausthal, pp. 417–481.
Estrin, Y., Mühlhaus, H.-B., 1996. From micro- to macroscale: gradient models of plasticity. In: Yen, W.Y.D., Broadbridge, P., Steiner, J.M. (Eds.), Australian Engineering Mathematics Conference. Sydney, 161–165.
Estrin, Y., Sluys, L.J., Brechet, Y., Molinari, A., 1998. A dislocation based gradient plasticity model. J. de Physique IV France 8, 135–141.
Fleck, N.A., Hutchinson, J.W., 1997. Strain gradient plasticity. Adv. Applied Mech. 33, 295–361.
Franciosi, P., Zaoui, A., 1982. Multislip in F.C.C. crystals: a theoretical approach compared with experimental data. Acta Metall. 30, 1627–1637.
Gao, H., Huang, Y., Nix, W.D., Hutchinson, J.W., 1999. Mechanism-based strain gradient plasticity – I Theory. J. Mech. Phys. Solids 49, 1239–1263.
Kubin, L.P., Poirier, J.-P., 1988. Relaxation oscillations and stick-slip of materials. In: Kubin, L.P., Martin, G. (Eds.), Non Linear Phenomena in Materials Science. Trans. Tech. Publ, Clausthal, pp. 473–482.
Lasry, D., Belytschko, T., 1988. Localization limiters in transient problems. Int. J. Solids Struct. 24, 581–597.
Lee, E.H., 1969. Elastic–plastic deformation at finite strains. J. Appl. Mech. Am. Soc. Mech. Engng. 36, 1–10.
Moran, B., Ortiz, M., Shih, C.F., 1990. Formulation of implicit finite element methods for multiplicative finite deformation plasticity. Int. J. Num. Meth. Engng. 29, 483–514.
Mühlhaus, H.-B., Aifantis, E.C., 1991. A variational principle for gradient plasticity. Int. J. Solids Struct. 28, 845–858.
Mühlhaus, H.-B., Boland, J., 1991. A gradient plasticity model for Lüders band propagation. PAGEOPH 137, 391–407.
Peirce, D., Asaro, R.J., Needleman, A., 1983. Material rate dependence and localized deformation in crystalline solids. Acta Metall. 31, 1951–1976.
Pijaudier-Cabot, G., Bažant, Z.P., 1987. Nonlocal damage theory. ASCE J. Engng. Mech. 113, 1512–1533.
Rice, J.R., 1971. Inelastic constitutive relations for solids: an internal-variable theory and its application to metal plasticity. J. Mech. Phys. Solids. 19, 443–455.

Sluys, L.J., 1992. Wave propagation, localisation and dispersion in softening solids. Doctoral thesis, Delft University of Technology, Delft.

Sluys, L.J., de Borst, R., Mühlhaus, H.-B., 1993. Wave propagation, localization and dispersion in a gradient-dependent medium. Int. J. Solids Struct. 30, 1153–1171.

Sluys, L.J., Ortiz, M., Needleman, A., 1995. Regularization by nonlocal dislocation effects in crystalline plasticity. In: Owen, D.R.J., Oñate, E., Hinton, E. (Eds.), Computational Plasticity, Fundamentals and Applications. Pineridge Press, Swansea, pp. 563–573.

Walgraef, D., Aifantis, E.C., 1985. On the formation and stability of dislocation patterns, I–III. Int. J. Engng. Sci. 12, 1351–1372.